

Yttria-stabilized zirconia as membrane material for electrolytic deoxidation of CaO–CaCl₂ melts

A. Martin · J. C. Poignet · J. Fouletier · M. Allibert ·
D. Lambertin · G. Bourgès

Received: 7 June 2009 / Accepted: 25 September 2009 / Published online: 11 October 2009
© Springer Science+Business Media B.V. 2009

Abstract This article is devoted to the study of the stability of an yttria-stabilized zirconia membrane used in the electrolysis of molten CaCl₂–CaO mixtures at 850 °C. Intensiostatic and potentiostatic electrolysis were carried for periods ranging from 10 to 20 h. Post-mortem composition profiles across the zirconia membrane were determined using Raman spectroscopy and microprobe analysis. The membrane degradation was analyzed in terms of synergetic parameters, i.e., chemical, electrochemical, and thermo-mechanical effects.

Keywords SOM technology · Zirconia · Deoxidation · Stability

1 Introduction

Worldwide commitments to reduce CO₂ emissions pose a formidable challenge. In this context, molten oxide electrolysis (MOE), which means electrolytic decomposition of molten metal oxide into metal and oxygen gas, represents an improvement over carbon thermochemical reduction processes or aluminum production by molten salt

electrolysis using consumable carbon anodes. Pyrochemical salt processes involving molten calcium, potassium, and sodium chlorides are also developed to prepare and purify plutonium. The two main advantages of these methods are the compactness and the rapid reaction kinetics. In the direct oxide reduction (DOR) process, plutonium dioxide and calcium are reacted in molten calcium chloride: plutonium dioxide is reduced to plutonium metal, while the calcium oxide by-product remains dissolved in the calcium chloride. This calcium oxide is ultimately converted back to calcium chloride in situ by bubbling chlorine gas through the molten salt. An alternative method is the direct electrolysis of calcium oxide, with calcium formation at the cathode of the cell and oxygen evolution at the anode. The main difficulties concern the selective oxidation of O²⁻ ions with respect to Cl⁻ ions oxidation, the corrosion of anode materials, the dissolution of the anodic gases in the electrolyte, and the solubility of calcium metal in the electrolyte. These difficulties can be theoretically avoided, using an oxide-ion conducting membrane that separates the anode from the melt containing the dissolved metal oxide. When the applied electric potential between the anode and the cathode exceeds the decomposition potential of the oxide to be treated, the cations are reduced at the cathode, the oxide ions migrate through the membrane and are oxidized at the anode. The solid oxide membrane (SOM) process has been proposed and patented as an alternative process for liquid metal deoxidation or extraction of metals, such as magnesium, titanium, tantalum, silicon, chromium, and aluminum from their respective oxides [1–4]. It has been shown that the process has to be conducted at temperatures between 1,100 and 1,300 °C. Several attempts have been made to employ oxide-ion conducting membrane anodes at temperatures below 1,000 °C. However, these efforts have

A. Martin · J. C. Poignet · J. Fouletier (✉)
University of Grenoble, LEPMI (INPG-UJF-CNRS), Phelma-Campus, BP 75, 38402 St. Martin d'Herès Cedex, France
e-mail: Jacques.Fouletier@lepmi.inpg.fr

M. Allibert
LPSC, 53, Av. des Martyrs, 38026 Grenoble Cedex 1, France

D. Lambertin
CEA Marcoule, SPDE, 30207 Bagnols sur Ceze, France

G. Bourgès
CEA Valduc, SRPU, 21120 Is sur Tille, France

not been successful in developing a commercially viable system mainly because sufficiently high current densities could not be obtained through the membranes. Stability of the membrane is also critical at these high temperatures. It has been observed that the loss of yttrium oxide from the membrane material is the dominant mechanism for membrane degradation. Similar observations have been reported for stabilized zirconia in steelmaking slags [5], molten glasses [6], and molten fluoride environment [7].

The purpose of this study is to electrochemically deoxidize CaO–CaCl₂ melts using a solid oxide membrane, i.e., yttria-stabilized zirconia, with a focus on the behavior of the interface between the ceramic material and the molten salt. No study has been performed up to now on the stability of stabilized zirconia in molten calcium chloride at 850 °C. The behavior of the membrane was studied under both potentiostatic and galvanostatic conditions.

2 Experimental

2.1 Experimental set-up

Figure 1 shows schematically the experimental cell, which consisted of two separate compartments. The cell temperature was maintained constant within 1 °C by a vertical Herman Moritz electrical furnace monitored by a regulator via a chromel–alumel thermocouple. The tube reactor was made from stainless steel, with a water-cooled top jacket and an O-ring airtight lid assembly containing appropriate holes for electrodes and ceramic membrane insertion and for gas circulation through the cell chamber. The alumina (Degussit AL23) crucibles were filled with dehydrated calcium chloride (Prolabo Normapur) and calcium oxide (Prolabo Rectapur) in appropriate proportions. An

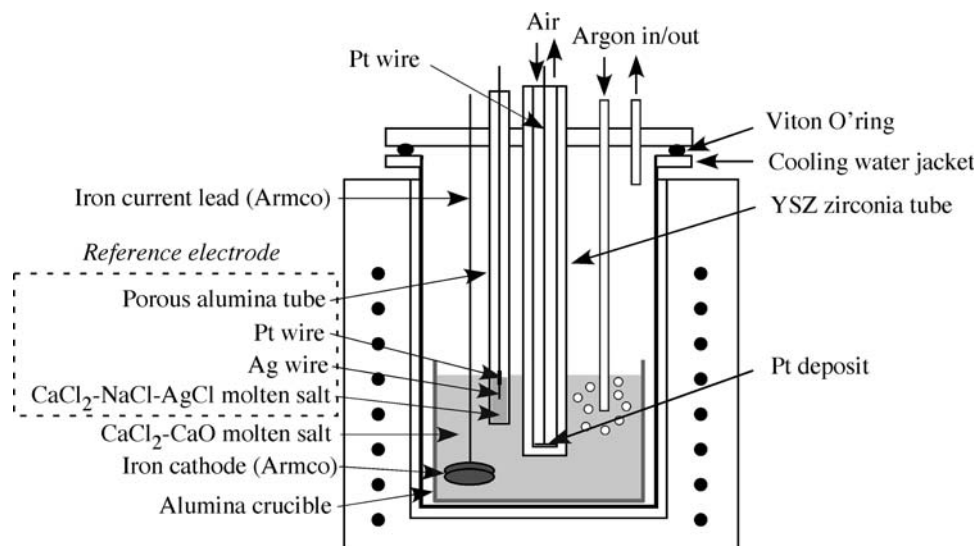
yttria-stabilized zirconia (YSZ) membrane was used as a separator between the anodic and cathodic compartments. It has been shown that the initial quality of the zirconia membrane is crucial to its operating life [8]. Consequently, the YSZ tube (8 mol%), with one end closed, was sintered in our laboratory at 1,623 K, starting from highly pure zirconia powder (Tosoh 8). It had a 10 mm outer diameter and a 1 mm wall thickness. The anode was a 0.4 cm² platinum layer (Engelhart Clal product: platinum ink 6082, 65% Pt), free from any other compound after baking, deposited on the inner surface of the bottom of the YSZ tube, in contact with ambient air during electrolysis. The cathode was an iron disk (Armco), 90 mm in diameter and 1 mm in thickness with a 1 mm in diameter Armco iron wire current lead (Armco iron contains less than 0.005% carbon). A reference electrode (referred to as Ag-Ref) was based on the Ag(0)/Ag(I) couple: a silver wire was immersed in the molten NaCl–CaCl₂ salt containing silver chloride (0.75 mol kg⁻¹) to fix a constant silver ion concentration; the reference molten salt was placed in the closed bottom of a porous alumina tube (Degussit AL24, 5% vol. porosity). A platinum wire, a few mm long, replaced the silver wire on both sides of the molten salt surface, to avoid risk of breaking of the silver electrode due to the temperature gradient at the liquid–gas interface. Purified argon, containing less than 1 ppm O₂ and H₂O, was flown through the reactor chamber at a rate of about 100 cm³ min⁻¹ during all the experiments.

Electrolyses were performed using a potentiostat/galvanostat PAR–EG&G controlled with M 270 software.

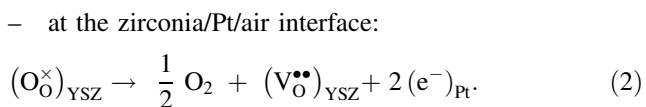
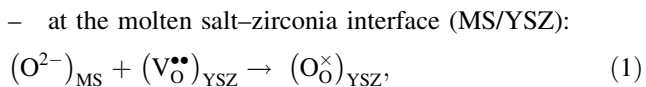
2.2 Experimental procedure

Electrolyses of CaCl₂–CaO mixtures were carried out either galvanostatically or potentiostatically. Assuming

Fig. 1 Reactor and electrolytic cell for cathodic deoxygenation of CaCl₂–CaO molten salt



that the zirconia membrane is a pure ionic conductor by O^{2-} ions, the interface processes on both sides of the zirconia tube can be schematized, using Kröger–Vink notation, as:



It has been shown previously [9] that, due to the large difference in ionic radii between Cl^{-} and O^{2-} ions, the reaction: $Cl^{-} + V_{O}^{\bullet\bullet} \rightarrow Cl_{O}^{\bullet}$ is kinetically highly unlikely. Consequently, provided a sufficient oxide-ion concentration is present at the molten salt–zirconia interface, the process corresponds to migration of O^{2-} ions (or of oxide vacancies in the other direction) through the zirconia wall. The oxide ions concentration in the molten salt at the interface with the oxide membrane determines a limiting current I_{lim} , corresponding to the highest O^{2-} ions flux through the interface. The electrochemical phenomena at the molten salt–zirconia interface depend on the operating modes.

Under galvanostatic experimental conditions, if the applied dc current is lower than $|I_{lim}|$, as illustrated in Fig. 2, the mass balance within a layer of the solid electrolyte near the molten salt–zirconia interface indicates that no stoichiometry change in the oxide occurs; only an oxide ions flux through the oxide electrolyte is observed: this flux J obeys the Faraday law, i.e., $J = I/2 F$ (where F is the Faraday constant). The cell works as an oxygen pump, with an evolving rate of oxygen equal to $I/4 F$ at the anode side of the cell. If the applied cathodic current I is higher than $|I_{lim}|$, which corresponds to the maximum oxide ions flux, the current obeys the following equation:

$$I = I_{lim} + I_e \tag{3}$$

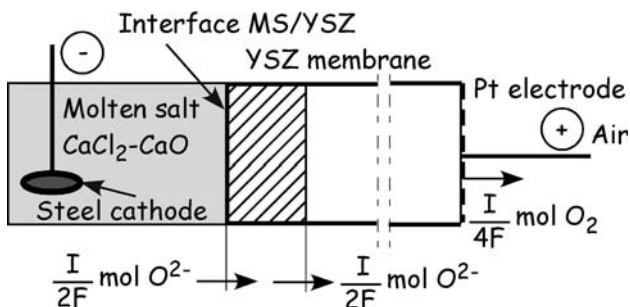


Fig. 2 Schematic representation of the interface process at the molten salt/solid oxide membrane interface (applied voltage less than the decomposition voltage of the oxide membrane)

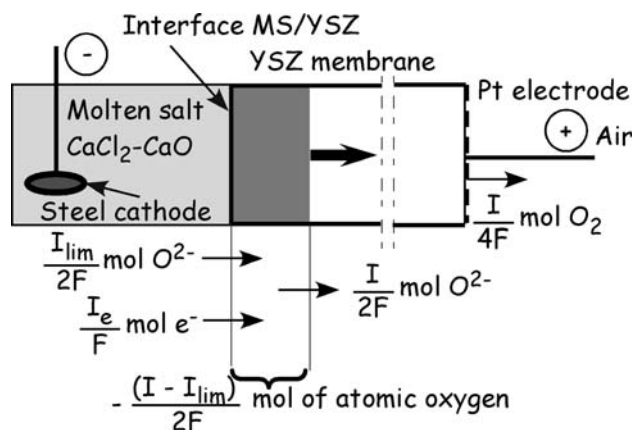


Fig. 3 Schematic representation of the interface process at the molten salt/solid oxide membrane interface (applied voltage higher than the decomposition voltage of the oxide membrane)

The current I_e corresponds to injection of electrons into the oxide electrolyte, inducing a black coloration. Basically, this partial reduction induces a valence change either of the cation (Zr^{4+} in the case of stabilized zirconia) or of a point defect (a dissolved chemical impurity or a structural defect such as an oxide-ion vacancy, i.e., formation of “color centers” such as V_{O}^{\bullet} or V_{O}^{\times}) [10, 11]. As shown in Fig. 3, the mass balance of oxide ions in a layer near the molten salt–zirconia interface demonstrates that the oxide material becomes non-stoichiometric [12]. It could be easily demonstrated that this non-stoichiometric zone progresses within the oxide material from the cathode to the anode [13, 14]. Consequently, as long as the reduced zone does not reach the anode of the cell, the oxygen flux evolving at the anode obeys the theoretical Faraday law; when the reduced zone reaches the anode, the yield of oxygen evolving decreases because the oxide becomes a mixed ionic–electronic material [15, 16].

Under potentiostatic conditions, if the absolute “net” applied voltage between both sides of the membrane (deducing the ohmic drop and the polarization phenomena) is sufficiently high to induce calcium oxide reduction, but lower than ca. 1.5 V/Air, no electrochemical reduction of the solid oxide electrolyte is observed and, either a stationary current is obtained, or the current tends to zero if the oxide-ion concentration in the molten salt is very low. If the absolute value of the voltage is higher than 1.5 V/Air, the electrolyte is electrochemically reduced and an increase of the current is observed. More precisely, as schematized in Fig. 2b, a reduced black zone progresses from the molten salt–zirconia interface toward the anode (zirconia/Pt interface). This reduced zone is a mixed ionic–electronic conductor, corresponding to a lowering of the ohmic resistance of the cell and of electrode polarizations. It has been shown, previously, that the reoxidation kinetics

of reduced zirconia under air is so high that the membrane can be broken [14]. Consequently, under potentiostatic mode, it is imperative to control the applied voltage in such way that the electrochemical reduction of the zirconia membrane be avoided. Both electrochemical modes have been used in this study.

3 Results

When the applied electrical potential between the anode and the cathode of the cell exceeds the decomposition potential of calcium oxide, Ca^{2+} ions are reduced at the cathode, the oxygen ions migrate through the membrane and get oxidized at the anode. In the previous article, we have reported that, when a sufficiently high voltage was applied between anode and cathode, we succeeded in producing pure oxygen gas with an anodic yield close to 100% [17].

Figure 4 gives an example of voltage variations at constant applied current density, i.e., 0.1 A cm^{-2} , over 18 h. Two steps were observed, corresponding to a noticeable increase of the anode potential, indicating an increase of the ohmic drop through the membrane. As discussed in the previous section, the electrochemical reduction of the oxide leads to a lowering of the solid electrolyte resistance. Consequently, the voltage increase observed cannot be ascribed directly to the electrochemical reduction of the oxide material but to a transformation of the membrane either at the molten salt–zirconia interface or within the ceramic membrane itself. The sudden increase of the voltage, associated with chlorine emission at the anode, indicated the breaking of the zirconia membrane. Moreover, the membrane part in contact with the molten salt became

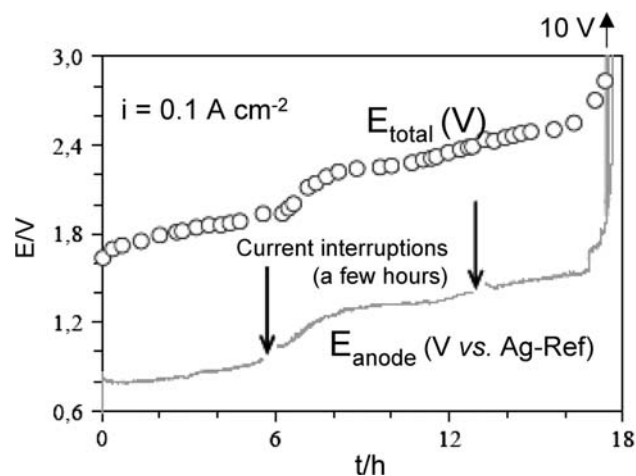
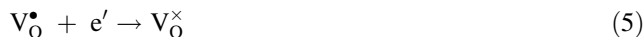


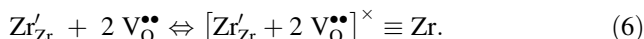
Fig. 4 Intensity-controlled electrolysis: variation of the cell voltage and of the anode potential versus Ag^+/Ag reference electrode; cathode: iron disk, molten salt: $\text{CaCl}_2\text{--CaO}$ (11 mol%); $i = 0.1 \text{ A cm}^{-2}$; $T = 840 \text{ }^\circ\text{C}$

black. It has been shown [10, 11, 13] that the electrochemical reduction of stabilized zirconia involves various processes:

- trapping of electrons on oxygen vacancies, with creation of F^+ and F color centers, according to:



- for more cathodic voltages, trapping of electrons on zirconium ions forming trivalent ions Zr'_{Zr} or even Zr''_{Zr} . The formation of zirconium metal atoms could result from the following reaction [18]:



Various authors have shown that the chemical stability of reduced-stabilized zirconia is dramatically lowered [19, 20]. Moreover, the reoxidation of F^+ and F color centers is reversible, but in the case of formation of Zr'_{Zr} or Zr''_{Zr} , monoclinic or quadratic zirconia is formed [11]. As indicated in the previous section, under galvanostatic electrolysis, the resulting voltage can become sufficiently high to cause electrochemical reduction of the zirconia membrane. In order to avoid this electrochemical reduction, potentiostatically controlled electrolyses were therefore carried out, with an applied net voltage below the electrochemical reduction limit.

The anodic potential was controlled and monitored versus the silver–silver chloride reference electrode. The OCV, $E_{i=0}$, was always ca. 0.4 V versus Ag-Ref. Eleven experiments were carried out, with four different molten salt concentrations, i.e., 12 mol% $\text{Li}_2\text{O--CaCl}_2$, 3 mol% CaO--CaCl_2 , 6 mol% CaO--CaCl_2 , and 6–9 mol% CaO--LiCl--CaCl_2 . A new zirconia membrane was used for each experiment.

Figure 5 shows the recorded current density after applying a polarization $\pi = E - E_{i=0}$ to the anode of the

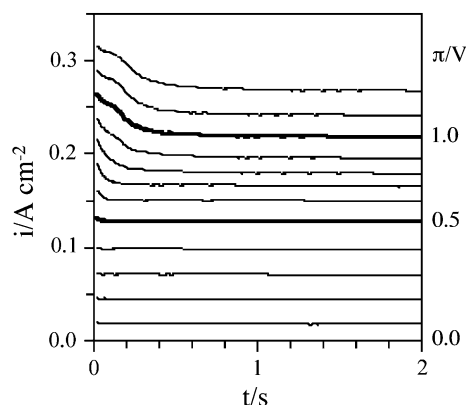


Fig. 5 Current density variation after applying an overpotential π (from +0.1 to +1.2 V), $T = 840 \text{ }^\circ\text{C}$

cell, from $\pi = 0.1$ V up to 1.2 V. Whatever the polarization, a stationary current density was obtained within <0.5 s. For a polarization of 0.4 V, the current density was ca. 0.1 A cm^{-2} , compatible with an industrial development. Figure 6 is plotted the polarization curves of 11 membranes in various molten salts. The current intensity was measured after 100 s polarization time. Within the experimental uncertainty ($\pm 5 \text{ mA cm}^{-2}$), quasi-linear curves were obtained indicating an ohmic control of the process. Moreover, the curves do not appear to depend on the oxide-ion concentration in the molten salt: the deoxidation yield will be the same at the beginning and at the end of the electrolysis. However, for longer electrolysis durations, we observed that, for a given polarization π , the current decreased progressively. This phenomenon started after the first 20 min. For $\pi = +0.9$ V, the current seemed to stabilize at an approximate value of 0.1 A cm^{-2} . For higher π values, it decreased down to zero. In both cases,

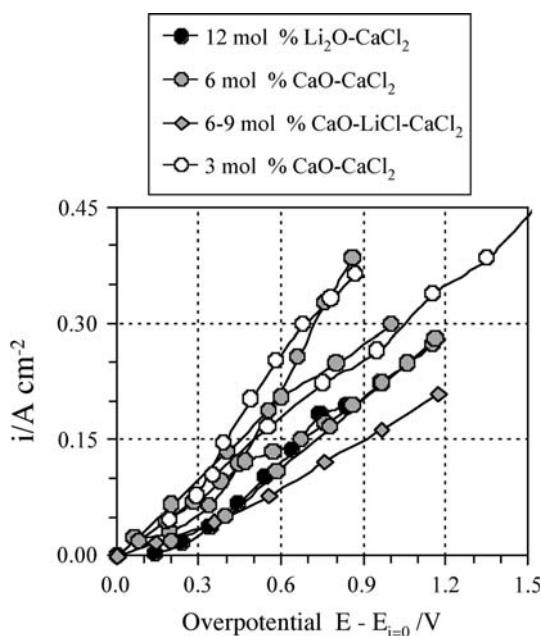
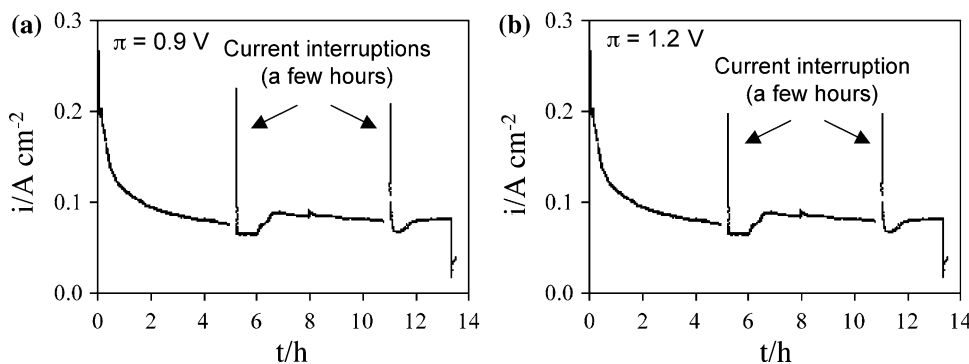


Fig. 6 Anodic polarization curves with fresh zirconia tubes for various molten salt compositions at $T = 840 \text{ }^\circ\text{C}$

Fig. 7 Variation of the current density as a function of the polarization, at $840 \text{ }^\circ\text{C}$ (a) $\pi = +0.9$ V; (b) $\pi = +1.2$ V



membrane breaking was observed after long time electrolysis, i.e. 15–20 h (Fig. 7).

Due to controlled applied polarizations, it can be assumed that there was no electrochemical reduction of the zirconia tube. As a matter of fact no gray–black color was observed on the immersed part of the zirconia membrane, even for 1.2 V polarization. However, even where the membrane appeared undamaged after the experiment, we observed that, a few days later, the tube became crumbly and broke up. This behavior could be ascribed to noticeable YSZ crystalline modifications. The compositional and structural profiles along the cross-section of the tubes, after long-term electrolysis, were determined by electron microprobe analysis and Raman spectroscopy. Figure 8 gives the variation versus time of the current density at constant polarization ($\pi = 0.9$ V), at $840 \text{ }^\circ\text{C}$ (Fig. 8a) and the yttrium profile within the zirconia tube, measured by electron microprobe analysis (Fig. 8b). The yttrium mole fraction within the membrane, near the anode of the cell, corresponds to the nominal mole fraction of the Tosoh powder. However, a large depletion of yttrium was observed from the interface between the membrane and the molten salt, to a depth larger than $300 \mu\text{m}$ in the oxide material. The structure along the cross-section of the zirconia tube was determined by Raman spectroscopy (spectrometer Dilor XY, wave length: 514.532 nm). Figure 9 compares the Raman spectra of the different zirconia phases (Fig. 9a) with the spectra obtained at the Pt/YSZ interface (Fig. 9b) and at the MS/YSZ interfaces (Fig. 9c), respectively. A noticeable modification of the zirconia structure was observed near the molten salt/membrane interface with appearance of monoclinic and tetragonal phases. Two examples of structure profiles are given in Fig. 10, corresponding to different electrolysis durations. The yttrium depletion went together with a destabilization of the zirconia phase: monoclinic, with traces of tetragonal phases were observed in the zones where the yttria content was below the nominal one. The structure modification extended within the membrane up to few 100 microns. It should be pointed out that these structural and chemical modifications were observed only in the bottom of the YSZ

Fig. 8 **a** Variation of the current density as a function of the polarization, at 840 °C, for a polarization $\pi = +0.9$ V. **b** Yttrium concentration, measured by EPMA, along the cross-section of the YSZ membrane after the electrolysis

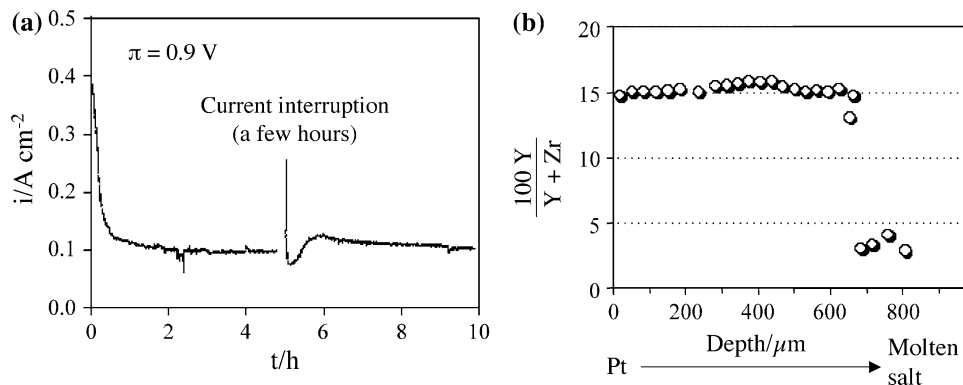
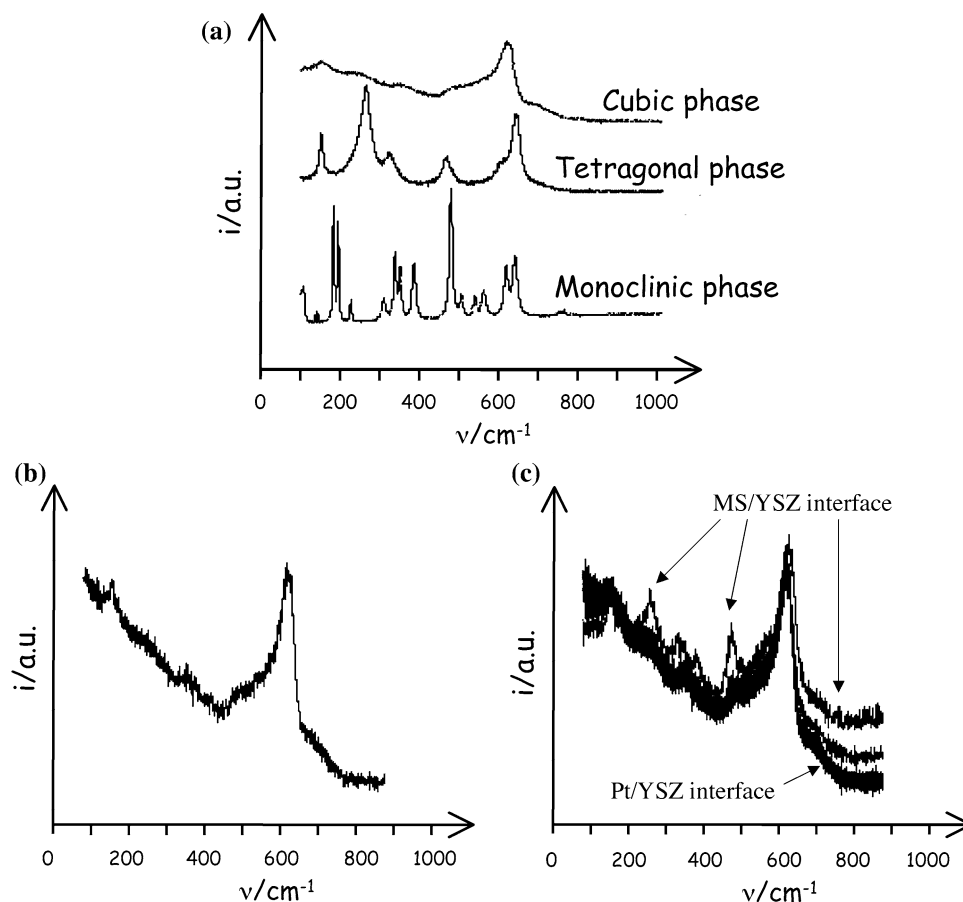


Fig. 9 Raman spectra of the zirconia tube. **a** Spectra of the different zirconia phases. **b** Raman spectrum at the Pt/YSZ interface. **c** Comparison between the spectra at the Pt/YSZ and the MS/YSZ interfaces, respectively



tube, and more precisely within the part of the material through which the current had passed.

4 Discussion

Various authors have observed a surface loss of yttrium from yttria-stabilized zirconia used in fluoride melts [21, 22], in molten sulfates [23], in molten sodium, and vanadium salts [24, 25], or in molten glasses [26, 27]. In these conditions, zirconia is no longer stabilized and

undergoes phase transformation leading to scaling off, formation of open porosity, and/or breaking of the membrane. The stability of zirconia has been studied either in static mode (oxygen sensors or thermal barrier coatings) or in galvanostatic mode (SOM processes) at temperatures generally significantly higher than 1,000 °C. It should be also pointed out that the ceramics used in the reported studies had very different purities, with a noticeable role of intergranular diffusion in materials of industrial purity.

The experiments reported, in this article, were carried out at 850 °C in molten calcium chloride, using stabilized

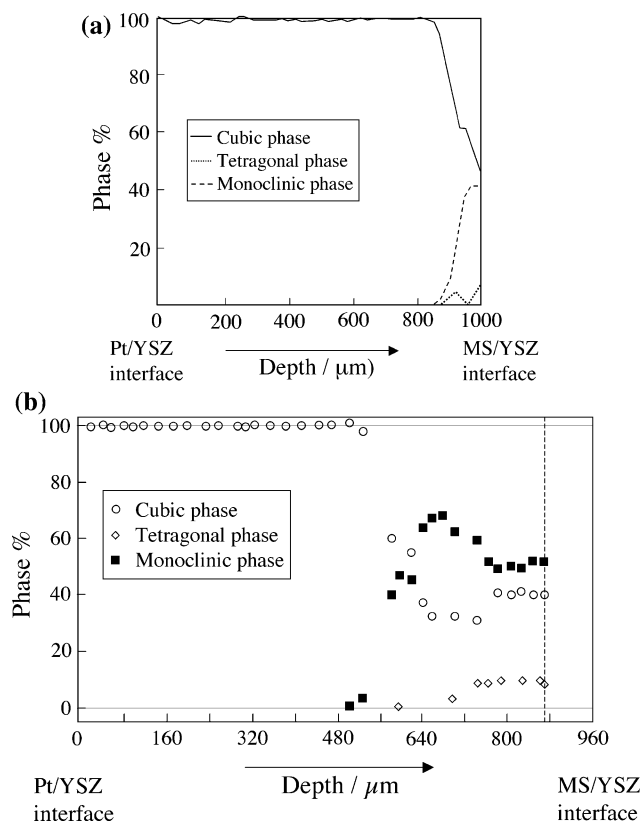


Fig. 10 Examples of concentration profiles of cubic, quadratic and monoclinic phases along the cross-section of the YSZ membrane after the electrolysis, determined by Raman spectroscopy

zirconia of high purity. When no current passed through the membrane, no damage was observed over several days. The membrane stability was affected by passing a direct current through the membrane during more than 10 h, even under controlled potential. The mechanism of reaction between the oxide membrane and the molten salt appears complex involving chemical, electrochemical, and mechanical processes.

The thermodynamical stability domain of the YSZ membrane can be studied using the oxobasicity concept. The potential–acidity diagrams of either calcia (see Fig. 11) or yttria-stabilized zirconias delineate the chemical and electrochemical stability domains of the membrane [28]. The oxidation limit corresponds to O₂ or Cl₂ evolution depending on the melt basicity. The reduction limit corresponds to the electrochemical reduction of the membrane. In oxoacid media, yttria can be dissolved, according to:



The acidic limit can be reached in the case of contact with oxoacidic compounds such as V₂O₅ that reacts with Y₂O₃ to form YVO₄ and causes the destabilization of zirconia ceramics. The stability of zirconia can be improved by

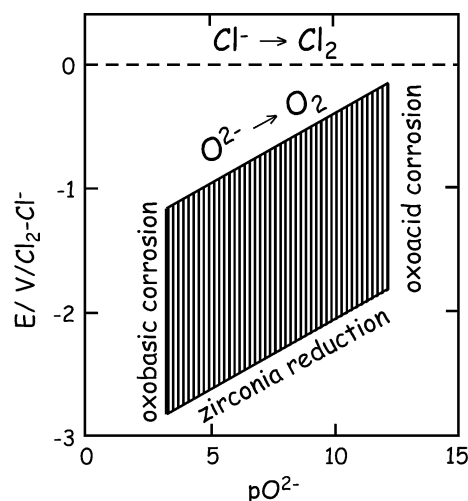
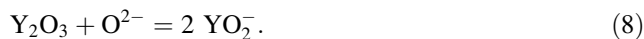
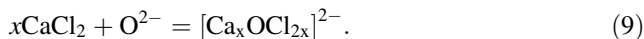


Fig. 11 Estimated oxoacidity diagram of calcia-stabilized zirconia, from Combes et al. [28]

substitution of Y₂O₃ with more acidic stabilizing elements such as CeO₂, In₂O₃, or Sc₂O₃. The molten salt used in the present experiments, CaCl₂–CaO, was oxobasic. In these conditions, the yttria stabilizer was liable to be dissolved, according to:



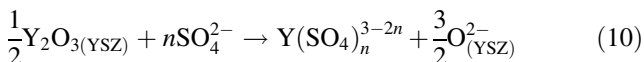
Using potentiometric titration in molten NaCl–KCl at 1,000 K, Combes et al. [29] demonstrated that this dissolution reaction is negligible for pO²⁻ higher than ca. 4 for calcia-stabilized zirconia (see Fig. 11) and about 6 for yttria-stabilized zirconia. Potentiometric determination of solubility products of alkaline-earth oxides in molten NaCl–KCl, at 1,000 K, using calcia-stabilized zirconia has been carried out by Combes et al. [30–32]. The determined corresponding pK_s (in molality scale) for MgO, CaO, and BaO were 9.0, 5.0, and 2.3, respectively. These authors assumed also the formation of complex ions, such as M₂O²⁺, or oxy-chloride complexes. More recently, Boghosian et al. [33] demonstrated that the high CaO solubility in calcium chloride could be ascribed to the formation of stable complexes with formula [Ca_xOCl_{2x}]²⁻, according to the following equilibrium:



The stability constant of the complex has been estimated by Boghosian et al. as superior as 10⁷. Therefore, due to the formation of stable complexes, the activity of free O²⁻ ions is small corresponding to pO²⁻ higher than the oxobasic corrosion limit of yttria-stabilized zirconia, i.e., pO²⁻ ca. 6. Consequently, in open circuit voltage, yttria-stabilized zirconia can be considered as chemically stable in the CaCl₂–CaO molten mixture. As an example, recent published results on corrosion of stainless steel coated with

300 μm thick yttria-stabilized zirconia confirmed that the YSZ coating exposed to molten LiCl–KCl eutectic salt did not reveal any significant attack and selective diffusion of elements even after 1,000 h of exposure [34].

As recalled previously, the stabilized zirconia stability is noticeably lowered when the oxide material is chemically or electrochemically reduced: in the reported experiments, the applied potential was controlled to avoid electrochemical reduction of the membrane. Nevertheless, a depletion of yttrium going hand in hand with destabilization of the zirconia membrane was observed at the interface with the molten salt. Windisch et al. [23] studied chemical processes at the interface between YSZ single-crystals and molten sodium sulfate using in situ Raman spectroscopy with the following cell: (–)Pt/Na₂SO₄/YSZ single-crystal/Pt(+). In experiments with anodic polarizations during a few minutes, an yttrium sulfate complex was detected in the molten salt close to the interface for current densities higher than 100 mA cm^{–2}. They suggested the possibility of an yttrium complexation by sulfate ions according to:



These authors proposed that yttrium ions migrate out of the ceramic oxide during anode polarization and form yttrium sulfate complexes. However, the yttrium depletion cannot be ascribed to cationic diffusion within the material because the yttrium diffusion coefficient is too low: to obtain a diffusion of yttrium over 100 μm in 10 h, the diffusion coefficient should be in the order of 10^{–13} m² s^{–1}. Weber et al. [35], using SIMS analysis have estimated the Zr⁴⁺ and Y³⁺ diffusion coefficients at 1,270 °C in yttria-stabilized zirconia: both coefficients are in the order of 10^{–20} m² s^{–1}. Moreover, this phenomenon could not be explained by a classical thermodynamical point of view and it was proposed that yttrium could be less stable near the single-crystal surface than in its bulk.

Figure 12 is plotted the impedance diagram at the open circuit voltage and under anodic or cathodic polarizations. The interface resistance is lowered with an anodic

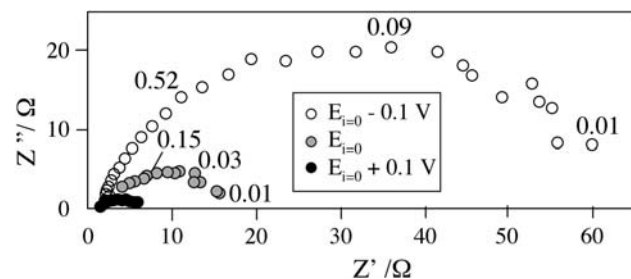


Fig. 12 Impedance diagram of the cell as a function of the polarization (applied alternative voltage: ± 0.02 V, frequency range: 10^{–2}–10⁴ Hz)

polarization compared with interface resistance determined at the OCV, indicating that the oxide-ion transfer through the interface does not seem to be the limiting process. The electrode resistance and electrode capacitance vary with the polarization according to: 63 Ω and 2.5×10^{-2} F, for –0.1 V polarization, 18 Ω and 9×10^{-2} F at open circuit, and 6 Ω and 2.5×10^{-1} F, for +0.1 V polarizations, respectively. Under potentiostatic anodic polarization, the oxide-ion activity close to the membrane surface becomes lower than the equilibrium activity at OCV, due to O^{2–} ions transfer from the melt into the zirconia membrane. The O^{2–} ions transferred from the molten salt within the membrane tend to be replaced, at the interface, by those arriving by both electrical migration and diffusion across the diffusion layer in the molten salt. The maximum value of the concentration gradient, which is reached when the oxide-ion concentration at the interface, [O^{2–}]_{int}, becomes zero, corresponds to a maximum current density i_{lim} . The following equation can be easily demonstrated, if the migrational part of the current can be neglected:

$$\frac{[\text{O}^{2-}]_{\text{int}}}{[\text{O}^{2-}]_{\text{o}}} = \frac{i_{\text{lim}} - i}{i_{\text{lim}}}, \quad (11)$$

where [O^{2–}]_o is the oxide-ion concentration in the bulk molten salt. The limiting current density i_{lim} obeys the Fick law:

$$i_{\text{lim}} = \frac{2FD_{\text{O}^{2-}}[\text{O}^{2-}]_{\text{o}}}{\delta} \quad (12)$$

where $D_{\text{O}^{2-}}$ is the diffusion coefficient of O^{2–} ions. The oxide-ion diffusion coefficient in CaCl₂–CaO molten salt has been determined by Ferro et al. [37] by measurement of the transport rate across a porous magnesia membrane. At 850 °C, the value of the oxide-ion diffusion coefficient reported by Ferro et al. was 2×10^{-5} cm² s^{–1}. The thickness of the diffusion layer δ across which there is a concentration gradient can be estimated in the order of 10 μm . As shown before, due to the formation of oxy-chloride complexes, the pO^{2–} value in the molten salt is in the order of 7–8. Using Eq. 12, the limiting current density can be estimated as 5×10^{-7} A cm^{–2}. Consequently, the observed current density, i.e., in the order of 0.1 A cm^{–2}, cannot be considered as resulting from free oxide ions diffusion. If the oxide-ion carriers are the complex ions ([Ca_xOCl_{2x}]^{2–}), assuming that all the dissolved calcium oxide is used for oxide complex formation, their concentration can be estimated as 10^{–3} mol cm^{–3}. Assuming that their diffusion coefficient is in the order of 5×10^{-7} cm² s^{–1}, the limiting current density can be estimated as 0.1 A cm^{–2}. The two main conclusions are the following: it can be assumed that the diffusion of the complex ions in the molten salt is the limiting step for the oxide-ion transfer through the YSZ membrane/molten salt interface and that,

for the present applied polarization (in the order of 0.4 V), the observed current density is equal to the limiting current density. Referring to the Nernst law, the oxide-ion activity at the interface will be very low, leading to a pO^{2-} value noticeably higher than the oxoacid stability limit of the YSZ membrane. Moreover, it should also be pointed out that, in these experimental conditions, due to interface heterogeneities between the membrane and the molten salt, significant local variations of the oxoacidity can be expected. Consequently, as illustrated schematically in Fig. 13, zirconia degradation is due to oxoacid attack (see also Fig. 11).

However, due to the very low diffusion coefficient of the yttrium ions in zirconias, the chemical reactivity cannot explain the expansion of this phenomenon from the surface within the bulk of the ceramics. With other authors [36], we observed that, after polarization, zirconia samples became brittle. This phenomenon can be ascribed to the volume expansion effect accompanying the cubic to monoclinic phase transformation ($\rho_{(ZrO_2\text{monoclinic})} = 5.81 \text{ g cm}^{-3}$, $\rho_{(YSZ\text{cubic})} = 5.97 \text{ g cm}^{-3}$). The molten salt infiltrates through the defects, such as microcracks and open pores within the ceramic membrane, leaching the stabilizer from zirconia, which induces the stabilizer depletion; consequently, the damaged region gradually expands from the molten salt/zirconia interface throughout the bulk of the material.

This process can also explain the breaking of the tubes few days after the experiment was stopped: the molten salt crystallizes out in the cracks and pores formed by destabilization, and its hygroscopicity leads to mechanical macroscale damage of the tube.

The stability of the YSZ membrane could be improved by adequate molten salt stirring [38], however, the limiting current density will not be increased dramatically. Likewise, due to the high complexing property of $CaCl_2$, the addition of calcium oxide in the molten salt, to maintain its

concentration near saturation, will not noticeably increase the limiting current. In order to minimize the dissolution of zirconia from the membrane, it has been proposed to add small amounts of yttria or of zirconia in the molten salt, so that their chemical potentials within the molten salt- and the yttria-stabilized zirconia membrane are identical [21, 39]. Finally, as suggested by Chen et al. [40], solvent exhibiting less complexing properties such as $BaCl_2$ could be an alternative, leading, at equilibrium, and under polarization, to a less oxoacid medium at the membrane/molten salt interface.

5 Conclusions

Deoxidation of $CaCl_2$ - CaO melts was carried out using a yttria-stabilized zirconia membrane. Current densities of ca. 0.1 A cm^{-2} with a polarization of 0.4 V was applied, at $850 \text{ }^\circ\text{C}$, for 20 h with a constant deoxidation yield. However, the membrane stability was affected by passing a direct current through the membrane, even under controlled potential. The mechanism of reaction between the oxide membrane and the molten salt appears complex involving chemical, electrochemical, and mechanical processes. Under anodic polarization, the yttria-stabilized zirconia degradation was ascribed to oxoacid corrosion.

Acknowledgments The authors wish to thank Marc Hénault (LEPMI-Phelma) for the fabrication of YSZ tubes.

References

1. Pal UB, Woolley DE, Kenney GB (2001) JOM October:32–35
2. Krishnan A, Lu XG, Pal UB (2005) Scand J Metall 34:293–310
3. Krishnan A, Lu XG, Pal UB (2005) Metall Mat Trans B 36 B:463–473
4. Pal UB, Powell AC IV (2007) JOM May:44–49
5. Schlesinger ME, Hagni RD (1992) TMS annual meeting, EPD Congress
6. Rodrigues CMS, Labrincha JA, Marques FMB (1998) J Eur Ceram Soc 18:2377–2381
7. Stournaras CJ, Tsetsekous A, Zambetakis T, Kontoyannis CG, Carouzos G (1995) J Mater Sci 30:4375–4379
8. Krishnan A (2006) Solid oxide membrane process for the direct reduction of magnesium from magnesium oxide. Ph.D. Thesis, Boston University
9. Fabry P (1976) Thesis, University of Grenoble
10. Fabry P, Kleitz M, Déportes C (1972) J Solid State Chem 5:1
11. Boulfrad S, Djurado E, Fouletier J (2009) Solid State Ionics 180:978–983
12. Fouletier J, Ghetta V (2009) In: Kharton VV (ed) Handbook of solid state electrochemistry, Chap. 12. Wiley-VCH, Weinheim, pp 397–420
13. Fabry P, Kleitz M (1976) In: Kleitz M, Dupuy J (eds) Electrode processes in solid state ionics. D Reidel, Dordrecht, pp 331–365
14. Fouletier J, Kleitz M (1975) Vacuum 25:307–314
15. Fouletier J, Kleitz M (1978) J Electrochem Soc 125:751–758

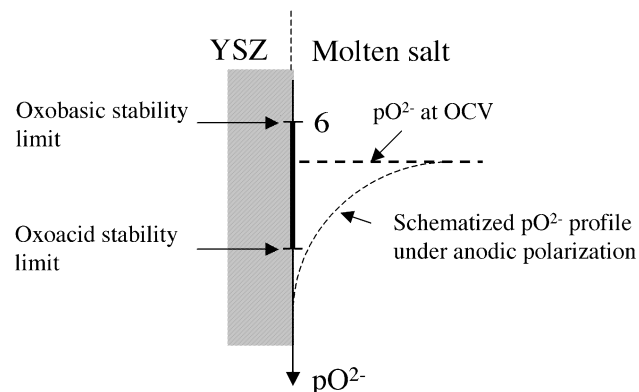


Fig. 13 Schematic variation of pO^{2-} at the YSZ membrane/molten calcium chloride interface, at OCV and under anodic polarization

16. Levy M, Fouletier J, Kleitz M (1980) *J Phys* 41:C6-335–C6-339
17. Martin A, Lambertin D, Poignet JC, Allibert M, Bourges G, Pescayre J, Fouletier J (2003) *JOM* October:52–54
18. Janek J, Korte C (1999) *Solid State Ionics* 116:181
19. Chatain D, Chabert F, Ghetta V, Fouletier J (1994) *J Am Ceram Soc* 77:197–201
20. Durov AV, Naidich YV, Kostyuk BD (2005) *J Mater Sci* 40:2173–2178
21. Krishnan A, Lu X, Pal UB (2005) In: Neelameggham N, Kaplan H, Powell B (eds) *Magnesium technology 2005*. The Minerals, Metals & Materials Society, Warrendale, pp 7–15
22. Kontoyannis CG, Carountzos G, Stournaras CJ, Tsetsekou A (1996) *J Mater Sci Lett* 15:222–224
23. Windisch CF Jr, Bates JL, Boget DI (1987) *J Am Ceram Soc* 70:C-220–C-221
24. Nagelberg AS (1985) *J Electrochem Soc* 132:2502–2507
25. Susnitzky DW, Hertl W, Carter CB (1988) *J Am Ceram Soc* 71:992–1004
26. Rodrigues CMS, Labrincha JA, Marques FMB (2000) *Solid State Ionics* 136–137:671–675
27. Rodrigues CMS, Labrincha JA, Marques FMB (1997) *J Electrochem Soc* 144:4303–4309
28. Combes R, Vedel J, Trémillon B (1975) *Electrochim Acta* 20:191–200
29. Combes RL, Koeller SL (2000). In: Rosenkilde C (ed) *Proc. Int. Symposium Jondal 2000*, pp 191–197
30. Combes R, De Andrade F, De Barros A, Ferreira H (1980) *Electrochim Acta* 25:371–374
31. De Andrade F, Combes R, Trémillon B (1975) *C R Acad Sci* 280:945
32. Combes R, Trémillon B, De Andrade F (1977) *J Electroanal Chem* 83:297
33. Boghosian S, Godø A, Mediaas H, Ravlo W, Østvold T (1991) *Acta Chem Scand* 45:145–147
34. Shankar AR, Mudali UK (2008) *Mater Corros* 59:878–882
35. Weber S, Scherrer S, Scherrer H, Kilo M, Taylor MA, Borchardt G (2003) *Appl Surf Sci* 203–204:656–659
36. Muqtader SA, Sidhu RK, Nagabhushan E, Muzaffaruddin K, Samdani SG SG (1993) *J Mater Sci Lett* 12:831–833
37. Ferro PD, Mishra B, Olson DL, Averill WA (1997) *Waste Manag* 17(7):451–461
38. Krishnan A, Lu XG, Pal UB (2005) *Scand J Metall* 34:293–301
39. Jones RL, Nordman DB, Gadowski ST (1985) *Metall Trans* 16A(2):303–306
40. Chen GZ, Fray DJ (2001) *J Appl Electrochem* 31:155–164